PROCEEDINGS OF THE INTERNATIONAL CONFERENCE ON THE PHYSICS OF SEMICONDUCTORS, KYOTO, 1966
JOURNAL OF THE PHYSICAL SOCIETY OF JAPAN VOL. 21, SUPPLEMENT, 1966

XII-4. Numerical Studies of a Two-Valley Model of the Gunn Effect

D. E. MCCUMBER

Bell Telephone Laboratories, Incorporated
Murray Hill, New Jersey, U.S.A.

The nonlinear partial differential equations of a two-valley model of Gunn-effect materials have been solved numerically for a variety of operating conditions. The results delineate different modes of sample response and indicate the microscopic transport configurations relevant to each. They also indicate the sensitivity of the different modes of operation to bias, contact impedance, and doping fluctuations. Hysteresis effects are predicted where the bias ranges of different modes overlap.

The nonlinear electron transport equations of a previously described[1,2] two-valley-conduction-band model of the Gunn effect in GaAs[2–4] have been solved numerically for a variety of operating conditions, and calculated dynamic electric-field distributions have been incorporated into a computer-generated movie which gives insight into the microscopic origin of observed effects.[5] While the model which we have studied oversimplifies transport in GaAs,[6,7] it is moderately tractable and incorporates the most important physical features—the basic negative differential conductivity, a field-sensitive diffusion coefficient, and retardation effects implicit in inervalley transfer. The results clearly demonstrate the relevance of space charge transport, and they predict hysteresis effects which have been seen in samples where several different modes of operation are possible.

The small-signal impedance $Z(\omega)$ of stably biased Gunn-effect materials can be expressed in terms of simple integrals which reduce to elementary analytic expressions for spatially homogeneous field distributions.[1,8,9] These expressions suggest that such materials are stable when driven from high-impedance constant-current sources but that they are possibly unstable when driven from low-impedance constant-voltage sources, conclusions which are supported by experiment and by the numerical calculations.[1,10] In what follows we shall be concerned exclusively with samples driven from zero-impedance constant-voltage sources.

Lightly doped samples (concentration-length product $n_0L \approx 10^{12}$ cm^{-2}) show an abrupt threshold for convective instability which is preceded by a range of lower bias for which the sample is small-signal stable but exhibits negative conductance in a band of frequencies near the average electron transit frequency $f_t = \bar{v}/L$ and possibly its harmonics. The bias regions for large-signal and small-signal stability may be different but overlapping; sample behavior in the overlap region depends upon bias history. The small-signal admittance depends upon the transit through the sample of space-charge waves which persist, in spite of the short dielectric relaxation time of the low-field material, because of the negative differential mobility (Fig. 2, ref. 2)) resulting from carrier intervalley transfer. Doping fluctuations influence the thresholds and the nature of possible instabilities, but they are not a prerequisite for negative conductance.

The rate of signal growth in convectively amplifying material biased in the negative-differential-mobility portions of the velocity-versus-field curve (Fig. 2, ref. 2)) increases approximately linearly with doping. As the concentration-length product n_0L increases above 10^{12} cm^{-2}, the bias range of stable small-signal negative-conductance operation decreases exponentially. For $n_0L > 10^{13}$ cm^{-2} such operation is practically impossible; stable positive-conductance operation is followed almost immediately at higher biases by large-amplitude Gunn oscillations.[3]

Shockley and Allen have suggested certain "equal-area" integral relations which govern the steady-state propagation of charge-dipole layers in long unstable samples.[11] Similar but more specialized relations were independently proposed by Butcher.[12] The equal-area relations are qualitatively useful in that they give physical insight into operating conditions, but they do not generally simplify quantitative calculations. Using a truncated version of the two-valley model[1] in which energy transport is neglected and the average carrier velocity is assumed to be an instantaneous function of the electric field plus diffusion, Copeland[13] has numerically computed steady-state properties of propagating accumulation, depletion, and dipole charge layers. Our results differ somewhat from Copeland's in the shape of the edges of the propagating high-field dipole domain (Fig. 1).

In moderately doped materials ($n_0 \geq 10^{15}$/cc) biased $\sim 10\%$ above threshold the rate of convective signal growth is so large that extremely small doping fluctuations are able to nucleate the formation of high-field dipole layers. Figure 17, ref. 1), shows the growth of such a layer in a

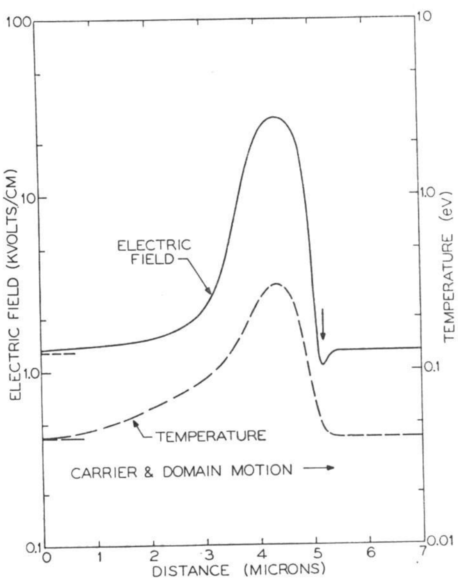

Fig. 1. Steady-state propagating high-field dipole domain in a long sample computed for GaAs with parameters (ref. 2)) $n_0 = 1.98 \times 10^{16}$/cc, $\Delta = 0.36$, $N_U/N_L = 60$, $\mu_L = 4200$ cm^2/V sec, $T_0 = 0.025$ eV, and $\tau_T = 3.55$ psec. The solid curve shows the electric field distribution (right scale). Note that the temperature and the electric field decay slowly at the trailing edge (left-hand side) but rise abruptly at the leading edge, the field rising from the small dip marked by the arrow. These results differ somewhat from those found by Copeland (ref. 13)) who assumed carrier mobility to be an instantaneous function of electric field, whereas in our calculations mobility is an instantaneous function of temperature but the latter is governed by a time-dependent energy transport equation. Time lags in the response of temperature and mobility to field become less relevant as the carrier density decreases and the diffusion-limited widths of the domain edges increase.

200 μm-long GaAs sample doped uniformly with $n_0 = 10^{15}$/cc except for a 1 μm perturbation 40 μm from the cathode contact in which the doping has been reduced by 0.01 per cent, the minimum fluctuation to be expected for a 1 μm length of typical laboratory-size crystals under the optimistic assumption that the doping impurities are uniformly distributed with Poisson statistics. Sensitivity to doping fluctuations varies exponentially with the concentration-length product $n_0 L$. The necessity for a minimum $n_0 L$ product for instability[14] is supported by the numerical calculations.[1,10]

Probe measurements[15] show that in many Gunn-effect devices the dipole layers are nucleated by a high-field region near a partially rectifying cathode contact rather than by doping fluctuations in the bulk of the sample. We have simulated finite-impedance ($E \neq 0$) partially rectifying contacts on a uniformly doped sample by an average reverse-bias mobility μ_R at the cathode source contact and an average forward-bias mobility μ_F at the anode sink contact. The computed stability properties of one such sample are summarized in Fig. 2. For this sample $\mu_U < \mu_R < \mu_L = \mu_F$, and the average mobilities $\bar{\mu}$ at the "peak" and "valley" of the velocity-versus-field curve (Fig. 2, ref. 2)) are $\bar{\mu}_m = v_m/E_m = 3460$ cm^2/V sec and $\bar{\mu}_2 = v_0/E_2 = 182$ cm^2/V sec, respectively.

For low and moderate bias—regions R_I, R_{II}, and R_{III} in Fig. 2—the field in the sample decreases from a maximum value at the cathode contact; the width of the space-charge partial-depletion layer at the cathode increases with increasing bias. As the bias increases from zero (region R_I), the current through the sample increases but gradually saturates. *Before* saturation is complete—that is, while dI/dV is still positive—the sample breaks into spontaneous oscillation (region R_{II}). The frequency of these oscillations is indicated in Fig. 2 and their nearly sinusoidal waveform is shown in Fig. 3. In region R_{II} a smooth, small high-field pulse cyclically forms near the cathode where the field is larger than the peak field E_m, propagates away from the cathode to fields less than E_m, and dissipates before reaching the anode. The behavior in region R_{III} is similar, except that alternate field pulses have different strength and different persistance. This is reflected in Fig. 2 by the near but not exact harmonic relation of the frequencies in R_{II} and R_{III} and in Fig. 3

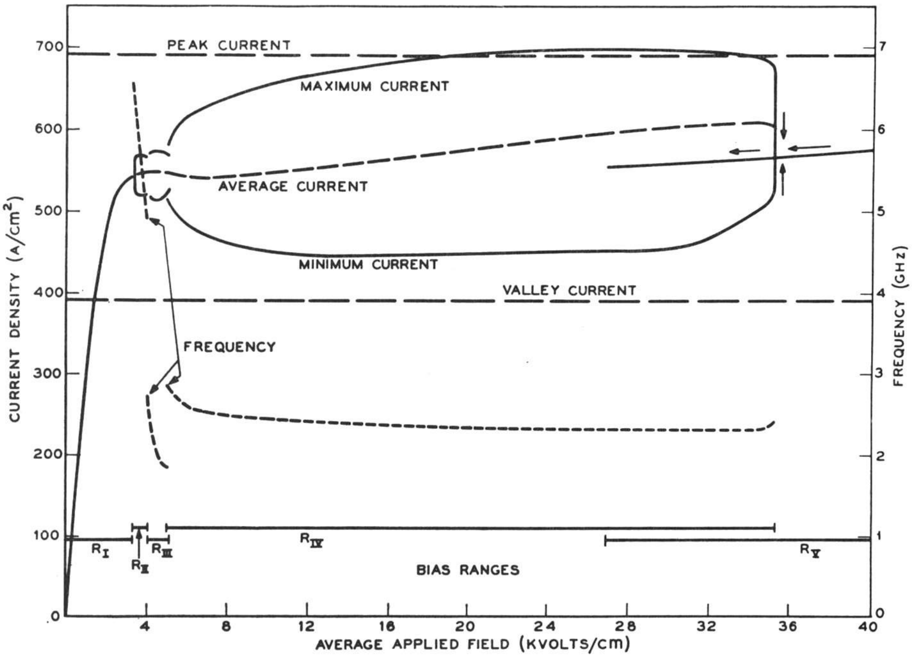

Fig. 2. Steady-state properties versus bias from a zero-impedance voltage source for a 50 μm sample of GaAs with parameters (ref. 2)) $n_0=4\times10^{14}$/cc, $\Delta=0.35$ eV, $N_U/N_L=60$, $\mu_L=5000$ cm²/V sec, $\mu_U=100$ cm²/V sec, $T_0=0.025$ eV, and $\tau_T=2$ psec. Partially rectifying contacts are approximated by an average reverse-bias mobility $\mu_R=1000$ cm²/V sec at the cathode source contact and an average forward-bias mobility $\mu_F=5000$ cm²/V sec at the anode sink contact. Five distinct bias regions R_j are apparent in the numerical results; hysteresis appears where the different regions overlap. In regions R_I and R_V the system is stable with a positive-resistance response. In regions R_{II}, R_{III}, and R_{IV} the system is unstable with the current oscillating at the indicated fundamental frequency (right scale) between the plotted extrema. For reference, the current corresponding to the "peak" and "valley" velocities of the velocity-versus-field curve (Fig. 2, ref. 2)) are also noted, as is the average (*dc*) current. Current waveforms are shown in Fig. 3.

by a R_{III} waveform which is similar to that in R_{II} but with alternate cycles "clipped." At the high-bias end of R_{III} alternate field pulses travel the full length of the sample to the anode contact. In the neighborhood of the I–II or the II–III "phase boundaries" steady-state behavior is tenuously maintained and transients decay much more slowly than for biases near the regions' centers.

At the low-bias end of region R_{IV} a single large-amplitude high-field dipole layer forms once each cycle at the cathode, propagates to the anode, and dissipates as a new dipole forms at the cathode. The current waveforms of Fig. 3 are similar to those previously computed for dipole instabilities[1,13,16] and to those measured by Fukui and Barber.[17] Hysteresis is observed at the R_{III}–R_{IV} boundary, where both R_{III} and R_{IV} behavior have been found for the same bias (5000 V/cm).

As the bias increases in R_{IV}, the high-field domain increases in width and a new domain is formed at the cathode well before the old domain has fully left the anode. More and more of the sample sees a high field until, at the high-bias end of R_{IV}, it is convenient to view the instability as a low-field domain moving in a high-field background, the low-field domain being the region between the forming and the dissipating high-field domains of the original picture.

As the bias is increased beyond R_{IV}, a single stable high-field domain fills the whole sample. As in R_I, the current in this new operating region R_V increases with increasing bias. Hysteresis is very conspicuous in the region of R_{IV}–R_V overlap and the operating point depends upon

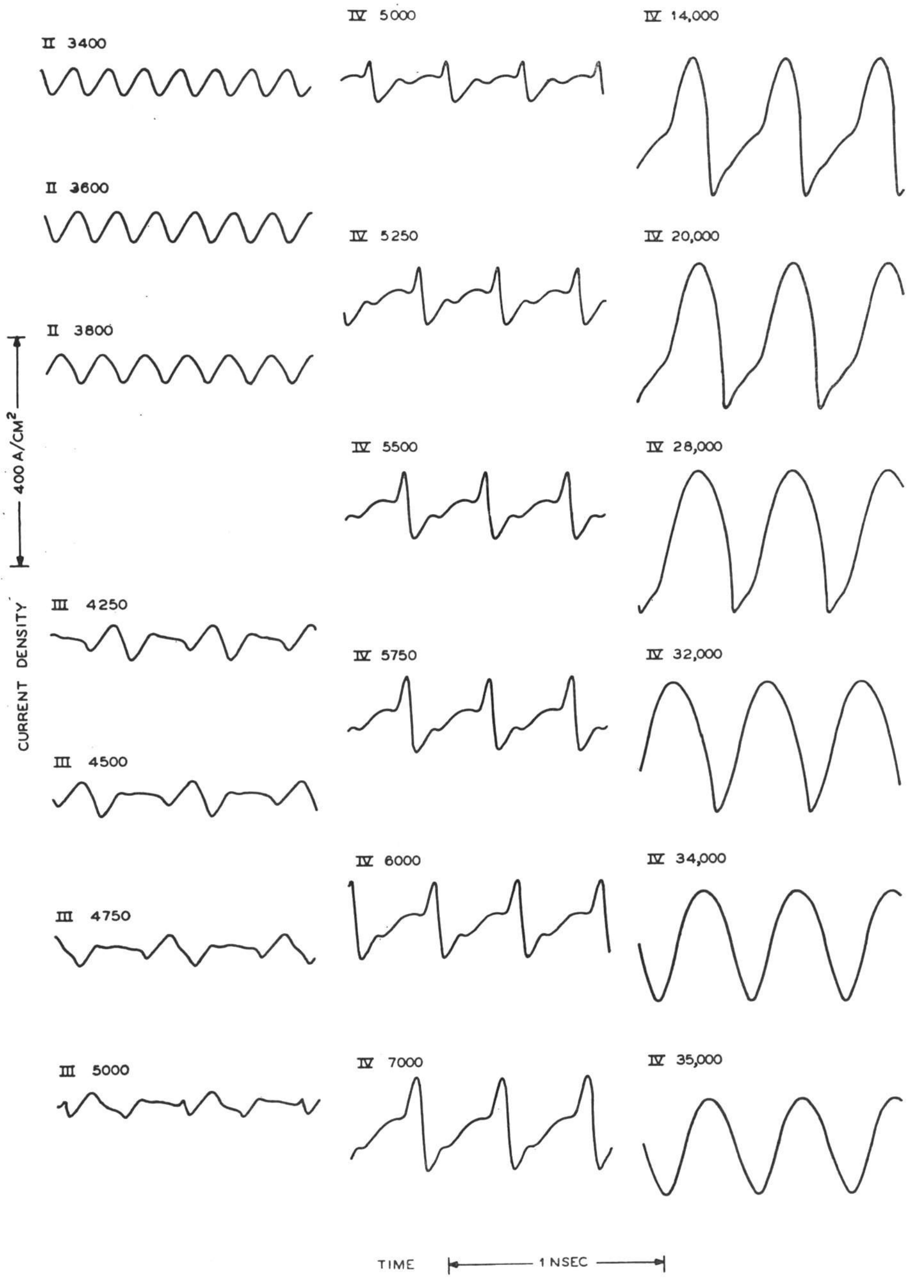

Fig. 3. Steady-state current waveforms for the oscillating modes of the system of Fig. 2. The bias region R_j is indicated by the Roman numeral, which is followed in each case by the average applied bias field in V/cm. Note the two distinct waveforms at 5000 V/cm where regions R_{II} and R_{III} overlap.

the rate at which the bias changes as well as upon the magnitude of those changes.

In summary, the numerical solutions, a number of which have been incorporated into computer-generated movies,[5] permit the identification of different modes of sample behavior and indicate the microscopic physical processes relevant to each.

The constructive suggestions of my colleagues have been very helpful throughout this work. I am especially grateful for interactions with, among many others, A. G. Chynoweth, M. R. Barber, J. A. Copeland, A. R. Hutson, W. L. Shockley, and M. Uenohara.

References

1) D. E. McCumber and A. G. Chynoweth: I. E. E. E. Trans. Electron Devices **13** (1966) 4.
2) A. G. Chynoweth, W. L. Feldmann, and D. E. McCumber: *Proc. Int. Conf. Semiconductor Physics*, Kyoto (1966) p. 514.
3) J. B. Gunn: I.B.M. J. Res. Dev. **8** (1964) 141; *Plasma Effects in Solids*, Paris 1964 (Dunod, Paris, 1965) p. 199.
4) Cf. I. E. E. E. Trans Electron Devices **13** No. 1 (January 1966).
5) The 16-mm movie "Dynamic Field Distributions in Gunn-Effect Devices" (September 1966) is available on loan from the Technical Information Library, Bell Telephone Laboratories, Murray Hill, New Jersey.
6) E. M. Conwell and M. O. Vassell: I. E. E. E. Trans. Electron Devices **13** (1966) 22.
7) P. N. Butcher and W. Fawcett: Proc. Phys. Soc. (London) **86** (1965) 1205.
8) B. W. Hakki: to be published.
9) W. L. Shockley, J. A. Copeland, and R. P. James: *Quantum Theory of Atoms, Molecules and the Solid State*, ed. P. -O. Lowdin (Academic Press, New York, to be published).
10) H. Kroemer: I. E. E. E. Trans. Electron Devices **13** (1966) 27.
11) *Quarterly Research Review No. 15, Stanford Electronics Laboratories* (Stanford University, Stanford, California, 1966) Vol. 2, p. 53.
12) P. N. Butcher: Phys. Letters **19** (1965) 546; P. N. Butcher and W. Fawcett: to be published in Brit. J. appl. Phys.
13) J. A. Copeland: to be published in J. appl. Phys. **37** (1966).
14) H. Kroemer: Proc. I. E. E. E. **52** (1964) 1736.
15) J. B. Gunn: private communication.
16) D. E. McCumber: NEREM Record **7** (1965) 76.
17) H. Fukui and M. R. Barber: Proc. I. E. E. E. **54** (1966) 785.

DISCUSSION

Hilsum, C.: What happens in a short sample—perhaps 10 microns long-that contains doping inhomogeneities ? Is it possible to get stable propagating accumulation layers ?

McCumber, D. E.: Our calculation indicates that samples with concentration-length products $N_0L \lesssim 10^{12}\text{cm}^{-2}$ are rather insensitive to quite large doping fluctuations. For such samples, contact effects seem to be much more relevant. As for propagating accumulation layers, these are found to exist only for $N_0L \gtrsim 5\times10^{12}\text{cm}^{-2}$. For smaller N_0L products the first accumulation layer stabilizes and forms a stable time-independent non-propagating field distribution. Unfortunately (for the observation of accumulation-layer modes of operation), the sensitivity of accumulation layers to doping fluctuations increases rapidly for N_0L above $5\times10^{12}\text{cm}^{-2}$.